Lawrence Berkeley National Laboratory

Title

Evaluating the Impacts of Weather Forecast Inaccuracy on Performance of Model Predictive Control for Dynamic Facades

Authors

Grant, Peter
Gehbauer, Christoph

Peer reviewed

Evaluating the Impacts of Weather Forecast Inaccuracy on Performance of Model Predictive Control for Dynamic Facades

Peter Grant[1] and Christoph Gehbauer[1]
[1]Lawrence Berkeley National Laboratory, Berkeley, CA

Abstract

Inaccuracy in weather forecasts and the impacts on predictive control systems are not yet well understood. This study evaluates weather forecast errors for U.S. Department of Energy reference cities and quantifies impacts on predictive control for dynamic facades. A stochastic noise algorithm emulated the forecast errors in simulation. Imperfect forecasts increased average electric cost by 13.3 % and glare index by 41.5 %, indicating that forecast error significantly decreases performance. However, bias correction largely mitigated the performance impacts to 0.0 % for electricity cost and 3.0 % for glare index. Future work developing practical bias-correction implementation methods is needed.

Introduction

Predictive control systems take weather forecasts into consideration when computing optimal control setpoints. These systems have the potential to (a) substantially reduce building energy consumption, (b) increase occupant comfort, and (c) support grid balancing goals (Killian and Kozek 2016). However, since they depend on weather forecasts they are sensitive to inaccuracies. Therefore, understanding the performance impact when provided with realistic, imperfect weather forecasts is critical.

Model Predictive Control (MPC) is a type of predictive controller that utilizes weather forecasts, mathematical system models, and an optimization algorithm to compute optimal setpoints for building devices. The prediction horizon is typically set between 1 to 24 hours, depending on the application. The setpoints are re-evaluated periodically as new building states and weather forecasts become available. One example of MPC is controlling dynamic facades to reduce building operating costs and associated emissions. The MPC must balance those energy goals with glare minimization, which is critical for occupant satisfaction. Prior research has shown that this approach can reduce building HVAC and lighting costs by 18.2 to 34.1 (median 27.1) % relative to standard windows with static interior shades (Gehbauer et al. 2020). Historical weather data is commonly used

when developing MPCs, but there can be large errors in real weather forecasts. This leads to the problem of developing a controller that performs well in the idealized case of using perfect weather forecasts, but may not perform as well in practical applications with imperfect weather forecasts.

The most advanced weather forecasting model available in the continental United States is the National Oceanic and Atmospheric Administration's (NOAA's) High Resolution Rapid Refresh (HRRR) model. It utilizes a 3 km^2 resolution, is updated hourly, and provides up to 48 hour forecasts (Weygandt 2009). HRRR forecasts still are not perfect. Griffin *et al.* found that HRRR tends to underpredict cloud cover early in the forecast horizon, and to have seasonal variations in prediction accuracy (Griffin et al. 2017). Lee *et al.* found that HRRR forecasts for Belle Mina and Cullman, Alabama were very accurate for surface air temperature ($R^2 < 0.95$), but not as accurate for solar radiation ($R^2 \cong 0.7$) (Lee et al. 2019). Rogers *et al.* compared HRRR solar irradiation forecasts to U.S. Surface Radiation Network (SURFRAD) data and found a relationship between irradiation forecast error and periods of maximum cloud variability (Rogers et al. 2012) (SURFRAD 2022). (Werth and Garret 2011) and (Hagedorn, Hamill, and Whitaker 2008) showed that most weather forecast error stems from the first hour of the forecast implying that bias correction, removing the error at the first hour from all hours in the forecast, can increase weather forecast accuracy.

Prior studies have demonstrated the potential for MPC to reduce building energy consumption. Siroky *et al.* demonstrated the potential for MPC by saving between 15 and 18 % on HVAC energy in a building on Czech Technical University Campus in Prague (Širokỳ et al. 2011) while assuming perfect weather forecasts. Dong and Lam developed and tested a nonlinear MPC in the Solar House at University of Texas which assumed perfect forecasts and demonstrated 30.1 % heating and 17.8 % cooling energy savings. Some prior efforts have explored the impacts of forecast error. Petersen and Bundgaard compared the performance of a simulated MPC with perfect weather forecasts to the same sim-

ulated MPC with real weather forecasts in Denmark, and found that MPC performance with imperfect forecasts was sensitive to thermal mass in the building (Petersen and Bundgaard 2014). Oldewurtel *et al.* developed a stochastic MPC designed to overcome the limitations of imperfect weather forecasts using chance constraints and affine disturbance feedback in the European context (Oldewurtel et al. 2012). Hedegaard *et al.* developed a method of estimating site weather data, enabling bias-correction of weather forecasts, using a combination of several nearby weather stations (Hedegaard et al. 2018). While Oldewurtel and Hedegaard present a valuable path forward, neither of them evaluated the uncertainty in weather forecasts from the HRRR model in the U. S. context, evaluated the impact of that uncertainty on MPC controlling dynamic facades, or quantified the improvements caused by bias-correction. Further, Hedegaard's solutions assumes that the weather measurements at nearby stations will be similar to on-site weather conditions, which may not be true for solar irradiation in areas with strong micro-climate effects or on partly cloudy days.

Methodology

This paper evaluates the impact of HRRR weather forecast error across 15 of the 16 U.S. Department of Energy (DOE) climate zones on the performance of an MPC controlling electrochromic windows. Fairbanks, Alaska was excluded because it is not currently available in pvlib's HRRR forecast tool (Holmgren, Hansen, and Mikofski 2018). Details describing the 15 studied climate zones are presented in Table 1. Cities are considered coastal or mountainous if they are within 50 miles of oceans or mountains. Due to the size of the Great Lakes and the fact that the HRRR model is still being enhanced in this region, cities at the Great Lakes are considered coastal for this paper.

The analysis consisted of the following three steps. First, the HRRR forecasts for each climate zone were compared to measured data, enabling quantification of the typical error in the HRRR forecasts. Second, a novel stochastic noise algorithm generating synthetic forecasts from historic weather data which are statistically equivalent to HRRR forecasts was created. Third, simulations using MPC were performed for the 15 climate zones using (a) *perfect* forecasts, i.e., no noise applied to simulated forecasts, (b) *stochastic* forecasts, i.e., synthetic noise algorithm applied to forecasts, and (c) *bias-corrected* forecasts, i.e., applied bias correction to stochastic forecasts. The three steps are described in the following subsections.

Table 1: Details of the 15 Studied DOE Climate Zones.

Climate Zone	Reference City	Time Zone	Geography
1A	Miami	Eastern	Coastal
2A	Houston	Central	Neither
2B	Phoenix	Mountain	Neither
3A	Atlanta	Eastern	Neither
3B-C	Los Angeles	Pacific	Coastal
3B	Las Vegas	Pacific	Neither
3C	San Francisco	Pacific	Coastal
4A	Baltimore	Eastern	Coastal
4B	Albuquerque	Mountain	Mountainous
4C	Seattle	Pacific	Coastal
5A	Chicago	Central	Coastal
5B	Boulder	Mountain	Mountainous
6A	Minneapolis St. Paul	Central	Neither
6B	Helena	Mountain	Mountainous
7	Duluth	Central	Coastal

Forecast Accuracy Evaluation

Predictive control systems for dynamic facades are primarily sensitive to the outdoor air temperature (OAT), global horizontal irradiation (GHI), and direct normal irradiation (DNI). To evaluate typical HRRR forecast error, the forecasts were retrieved using pvlib's HRRR interface and compared to measured weather data for each site. The HRRR forecasts were recorded at each hour for each of the reference cities from May 19, 2021 to March 31, 2022. Those dates cover the time period from the start of the study to the submission of this paper. NOAA's HRRR model provides OAT and cloud cover data. pvlib was used to convert cloud cover to irradiance by assuming a linear relationship between cloud cover and GHI ranging from the clear sky GHI to a minimum GHI threshold as described in (Larson 2016). The pvlib module then uses the DISC model to calculate DNI (Maxwell 1987). The measured weather data was obtained through DarkSky (DarkSky 2021). Weather data from DarkSky also returns OAT and cloud cover which was converted to irradiance using pvlib's cloud cover to irradiance algorithm.

To quantify the error in the forecasts, the relative error for OAT, GHI, and diffuse horizontal irradiation (DHI) were calculated for each hour of the 16 hours in the forecast, and all forecasts in the data set. The relative error was calculated using Equation 1 where X is the weather parameter of interest in each calculation. This calcula-

tion was performed for each hour in the available forecasts. Calculations around sunrise or sunset, when the forecast solar irradiance is very low, can result in extreme relative errors. To avoid this issue the data was filtered to times when both forecast and observed GHI were above 10 W/m^2 for all irradiance calculations. Similarly, the relative error in OAT was calculated using degrees Kelvin to avoid high relative errors when OAT is close to zero degrees Celsius. The relative error identified during each hour of the forecast was then added to a dataset tracking the error metrics for that hour of each forecast. For example, a dataset tracking the error in the third hour of HRRR forecasts contained the error in forecasted weather at 15:00 from forecasts released at noon. These datasets were used to obtain the bias and standard deviation in forecast error for each weather parameter at each hour of the forecast, e.g., error at the first hour in the forecast, second hour in the forecast, and so on. A separate dataset was created for each climate zone. These metrics are referred to as *non-temporal error* in this paper.

$$X_{RelativeError} = (X_{Forecast} - X_{Observed})/X_{Forecast} \quad (1)$$

The change in relative error between any two successive hours was also calculated and added to datasets tracking the temporal change in error metrics for each forecast. For example, a dataset tracking the temporal change in error between the third and fourth hours of the forecast contained the temporal change in forecast error between 15:00 and 16:00 for the forecast released at noon. These datasets were used to obtain the standard deviation in temporal error change for each parameter at each hour of the forecast. A separate data set was created for each climate zone. These metrics are referred to as *temporal error* in this paper.

The bias and standard deviation metrics were calculated across the 15 studied DOE reference cities to evaluate the performance of the HRRR model. Reference cities were grouped and examined by time zone, proximity to coasts, and proximity to mountainous regions. Table 1 presents geographical characteristics of the location of each city.

Stochastic Algorithm Development

A novel stochastic noise algorithm was developed to synthetically generate weather forecasts with statistically equivalent properties to real HRRR forecasts using a weather forecast and city as inputs. It provides the option to use bias-corrected forecasts which applies an offset to the weather forecast equal to the difference between the current weather measurements and forecast.

Bias-correction is only possible if local weather measurements are available. The algorithm uses the calculated error metrics to represent the typical error in the HRRR forecast for each reference city using the following five steps.

1. Generate an initial starting point for the error profile. If bias correction is applied then the stochastic noise at the time that the forecast begins (hour zero) is zero. If bias correction is not applied then a stochastic noise multiplier for hour zero using the computed non-temporal bias and standard deviation at hour zero is used. The bias and standard deviation metrics were identified for each climate zone in the forecast accuracy evaluation. The algorithm performs these calculations for OAT, GHI, and DHI.

2. Project the change in forecast error between each hour of the forecast. The change in error between hours is generated from a normal distribution representing the temporal error metrics identified in the forecast accuracy evaluation. These temporal errors are then combined to identify the projected error in each hour of the forecast. This profile is then added to the error at hour zero. The algorithm performs these calculations for OAT, GHI, and DHI.

3. Compare the relative errors of the generated forecast to the ones from the observed HRRR data. Any point where the relative error exceeded three standard deviations of typical non-temporal error is considered an outlier, and the whole profile is rejected. When a profile is rejected the stochastic algorithm generates a new profile using a different seed for the same time period, starting at step 1.

4. Apply the generated error profile to the provided historic weather data to generate the weather forecast with equivalent uncertainty to real HRRR forecasts.

5. Calculate the DNI from the stochastic GHI and DHI using pvlib's DNI calculation function.

Figure 1 demonstrates steps one to three of creating a GHI error profile for San Francisco, CA without bias correction. The top subplot shows the error generation process. The error at hour zero is estimated by generating a random number in a normal distribution defined by the statistics of the observed HRRR data. This is represented by the blue dot, and is 16 % in this example. The red dashed lines show the ±3 standard deviations limit for each hour. The standard deviation in change of relative

error between hours zero and one for GHI in San Francisco is 22 %. The green area highlights an error change of ± 66 % (3 standard deviations), indicating the possible range of forecast error at hour one. The stochastic algorithm generates the error for hour one by choosing a random number in the range shown in the green region. The algorithm repeats this process for all hours in the forecast to generate the error profile. The green dashed line in the bottom subplot shows the error profile generated by the stochastic algorithm. Since none of the points in the error profile are outside the ±3 standard deviation limits, the stochastic algorithm accepts this profile and generates the synthetic forecast. If on-site measurements are available, enabling bias correction, the 16 % relative error in hour zero is subtracted from each point.
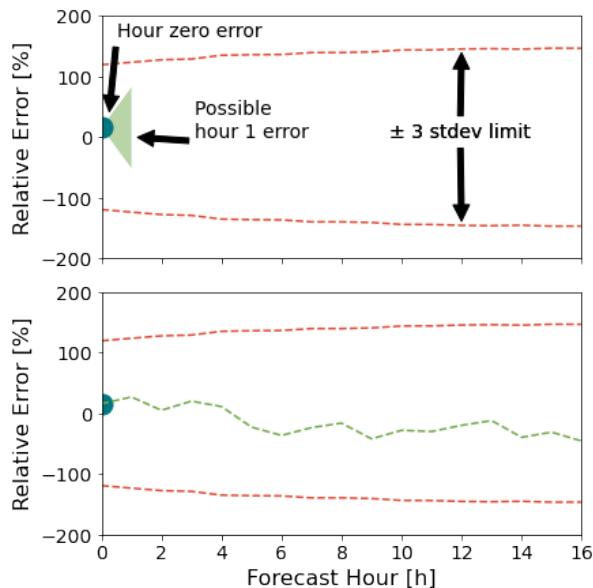

Figure 1: Example Synthetic Noise for Global Horizontal Irradiance Forecast in San Francisco, CA.

MPC Performance Impact Simulations

The project team utilized simulations predicting the performance of an MPC controlling a vertically divided three-zone electrochromic window in a 14 m² south-facing private office with a 60 % window to wall ratio. The simulation setup was previously introduced in (Gehbauer et al. 2020). Simulations for the first week of each month used perfect, stochastic, and bias-corrected weather forecasts. The MPC used a one hour prediction horizon and re-optimized every five minutes. The simulation setup used Typical Meteorological Year (TMY) historic weather data for both the weather forecast and actual weather data. To enable simulations with imperfect weather forecasts the simulation setup was modified to pass the TMY data through the developed stochastic forecast algorithm. This process created a forecast with errors which was then provided to the MPC. Simulations with and without weather forecast uncertainty enabled direct comparison of MPC performance. Simulation results were evaluated to determine the impact of (a) stochastic forecasts and (b) bias-corrected stochastic forecasts on MPC performance in terms of (a) total electricity cost using a time-of-use electricity tariff, (b) typical glare level calculated using RADIANCE, and (c) daylight ratio from daylight in the room. All evaluations are expressed in terms of the percent change of the parameter on a weekly basis using the perfect forecast as the baseline.

Results

The results of the forecast error evaluation and the effect of weather forecast inaccuracy on MPC performance are presented in individual subsections.

Forecast Accuracy Evaluation

Figure 2 presents the non-temporal GHI error for each climate zone averaged across the entire data set for each of the 16 hours in the HRRR forecasts. Dashed lines represent cities in coastal climate zones, dotted lines represent cities in mountainous climate zones, and solid lines represent the rest. The error generally increases as the forecast hour increases. The relative error is higher for 5B (mountainous), 6B (mountainous), 7 (coastal), and 3B-C (coastal) than for the other climate zones. While most error metrics are in the range of 35 to 59 %, the metrics for those four climate zones are in the range of 61 to 80 %.

Figure 3 presents the same information for OAT. The non-temporal error is significantly smaller for OAT than for GHI. The OAT relative error calculation used degrees Kelvin, avoiding points where the denominator approached zero. To provide context 1 % relative error at 293.15 degrees Kelvin (20 degrees Celsius) is 2.93 degrees Kelvin/Celsius. The non-temporal error for OAT ranges from 0.7 to 1.6 % depending on the forecast hour and climate zone. There is no discernible pattern indicating that relative error in OAT increases in either coastal or mountainous regions.

Figure 4 presents the temporal error in GHI forecasts for each climate zone. The x-axis values match the hour at the end of the error change. For example, the data at hour one indicates the standard deviation in change of relative error between forecast hour zero and forecast
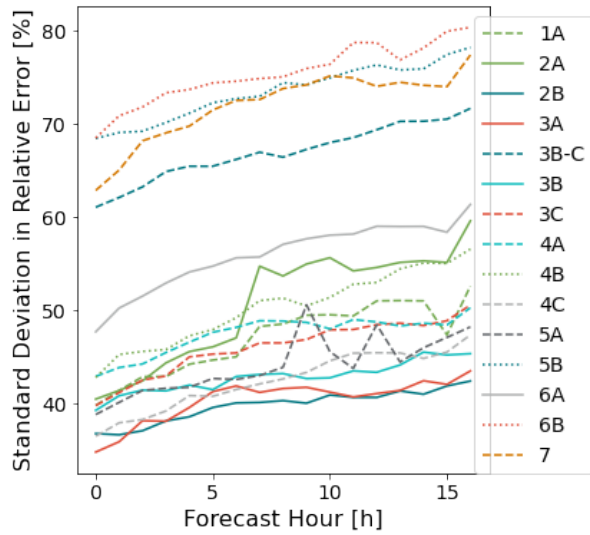
Figure 2: Standard Deviation in Global Horizontal Irradiation Relative Error for Each Climate Zone.

Figure 3: Standard Deviation in Outdoor Air Temperature Relative Error for Each Climate Zone.

hour one. The standard deviation typically increases with each hour in the forecast, though this effect is muted when compared to the non-temporal data set. The climate zones with the most variability in forecast error are 6B (mountainous), 5B (mountainous), 7 (coastal), and 1A (coastal). This difference is again muted when compared to the non-temporal data set. 6B, 5B, and 7 were also among the four climate zones with the highest GHI forecast error in the non-temporal data set. 1A replaced 3B-C.

Figure 5 presents the same information for OAT. The standard deviation for each climate zone is typically very steady until hour nine or ten, depending on the climate zone. At that time the standard deviations increase dramatically. This indicates that the error in HRRR temperature forecasts becomes less predictable after hour nine or ten. Averaged across the 16 hours, the four climate zones with the most variation in temporal error are 4B (mountainous), 2B (neither), 5B (mountainous), and 3B (neither).

MPC Performance Impact Simulations

Table 2 presents the average and standard deviation (formatted: average / standard deviation) percent change in each error metric. As previously stated the error metrics are electric charge, glare index, and daylight ratio. Each metric is evaluated on a weekly basis and presents the change in predictive controller performance when using stochastic instead of perfect forecasts. Each
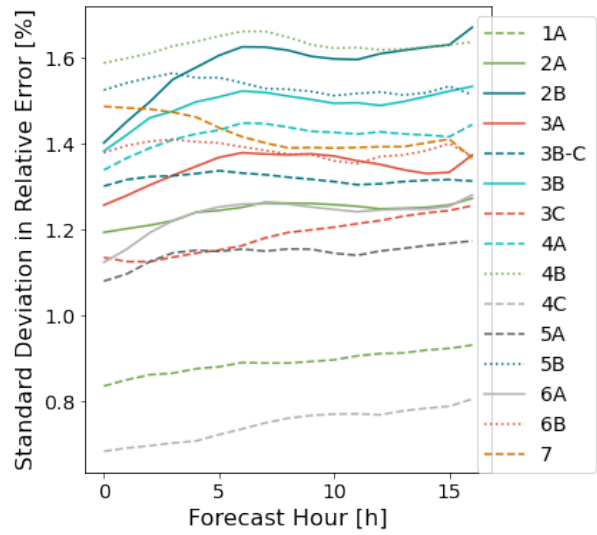
row provides data for the specified climate zone, except for "All" which provides the impacts across all climate zones. Overall the analysis revealed a 13.3 % increase in electric charge, 41.5 % increase in glare index, and 119.3 % increase in daylight ratio when using the stochastic forecasts. The maximum increase in electric cost was 36.9 % in climate zone 6B. The maximum increase in glare index was 118.5 %, in climate zone 5B.

The three climate zones with the largest performance impacts for each parameter are highlighted in bold font. 5B, 6B, and 7 showed the largest impacts in electricity cost. 3B-C, 5B, and 6B showed the highest impacts for glare index and daylight ratio. Figure 2 showed that the four climate zones with the highest non-temporal error in GHI were 3B-C, 5B, 6B, and 7, which likely caused the high impacts in the most impacted climates.

Table 3 presents the average weekly percent change between MPC simulation results with bias-corrected stochastic forecasts and perfect forecasts. The data set showed average changes of 0 % in total electric charge, 3.0 % in glare index, and 3.4 % in daylight ratio. The maximum increase in electric cost was 0.4 % in 2B and the maximum increase in glare index was 4.8 % in 3A.

The three climate zones with the largest performance impacts for each parameter are again highlighted in bold. The data set with bias correction shows more diversity. 2B, 4B, and 4C show the highest impacts in electric charge. 1A, 3A, and 4C show the largest average increase in glare index. 6A, 6B, and 7 show the largest
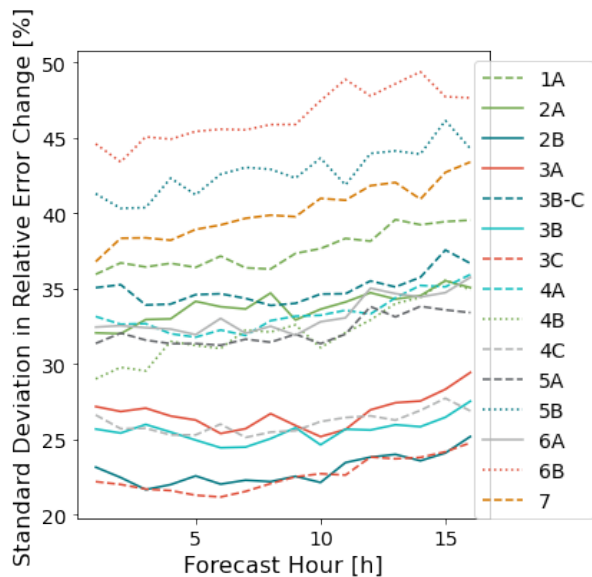
Figure 4: Standard Deviation in Hourly Change of Global Horizontal Irradiation Relative Error for Each Climate Zone.

Figure 5: Standard Deviation in Hourly Change of Outdoor Air Temperature Relative Error for Each Climate Zone.

impacts in daylight ratio.

Discussion

The accuracy of non-temporal GHI forecasts from NOAA's HRRR forecast model vary with climate zone. Forecasts for climate zones 5B, 6B, 7, and 3B-C (two mountainous, and two coastal) all showed significantly higher error than the others. The errors for those zones ranged from 61 to 80 %, compared to 35 to 59 % for all other climate zones. This work expands Lee *et al.*'s findings from specifically Alabama to the contiguous United States, with a focus on the DOE reference cities commonly used for building energy simulation studies.

This work presents a novel stochastic noise algorithm that replicates the error in weather forecasts utilizing the statistics derived from the weather forecast analysis.

Further work could lead to a more accurate representation during certain conditions. Currently all valid hours in all forecasts are lumped into a single group. This could be improved in the following ways:

- Low irradiation values around sunrise and sunset lead to small errors returning large relative errors. Combining all hours into a single dataset averages this effect across the full day, neglecting the diurnal variation. Different datasets for these two time periods could yield more accurate statistics.
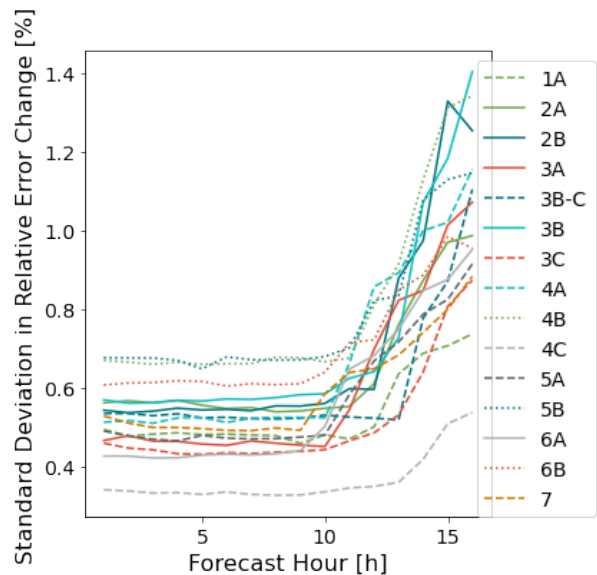
- Prior research indicated that HRRR accurately evaluates irradiation during either sunny or cloudy conditions but sometimes erroneously predicts clouds, which drives errors in the irradiation forecasts. Future work should evaluate the accuracy of HRRR on cloudy, partly cloudy, and sunny days then apply different statistics depending on the predicted cloudiness level.

- Preliminary data analysis implied that HRRR tends to overestimate OAT during the day and underestimate OAT at night. Further evaluation of this trend could determine whether or not it really occurs, create different statistics for daytime and nighttime, and use the different statistical values to more accurately predict daytime/nighttime OAT error.

Inaccuracy in weather forecasts clearly decreases the performance of MPC for dynamic facades. Simulations in 15 U.S. climate zones, showed that the stochastic forecasts increased the total electric cost by 1.5 to 36.9 % depending on the climate zone. The increase in electricity cost decreases the cost-effectiveness of MPC. The predicted average glare index increased by 7.4 to 118.5 % depending on the climate zone. The increase in glare would likely be too high for occupant satisfaction and decrease acceptance of MPC.

Simulations using MPC with bias-corrected forecasts

Table 2: Average and Standard Deviation Change in MPC Performance with Stochastic Forecasts

Climate Zone	Electric Charge [%]	Glare Index [%]	Daylight Ratio [%]
1A	1.5 / 0.9	18.5 / 11.3	22.7 / 13.1
2A	1.5 / 1.2	16.8 / 16.3	27.5 / 22.6
2B	15.6 / 11.7	42.1 / 22.6	159.2 / 167.8
3A	2.0 / 2.2	42.1 / 7.3	15.8 / 17.2
3B	10.3 / 9.9	33.4 / 21.8	103.9 / 81.8
3B-C	18.8 / 13.2	**96.4 / 56.0**	**209.9 / 103.7**
3C	7.6 / 10.6	23.0 / 18.3	44.1 / 40.9
4A	5.5 / 3.6	25.1 / 12.3	69.3 / 74.8
4B	22.5 / 21.1	56.4 / 32.7	164.3 / 130.2
4C	4.7 / 6.3	15.5 / 11.3	27.1 / 21.0
5A	3.5 / 4.6	7.4 / 7.5	42.4 / 38.1
5B	**35.3 / 14.9**	**118.5 / 52.4**	**331.2 / 292.5**
6A	9.3 / 6.9	20.1 / 14.1	92.2 / 116.8
6B	**36.9 / 17.9**	**92.9 / 48.2**	**315.6 / 270.9**
7	**24.9 / 21.1**	46.2 / 23.3	164.9 / 159.6
All	13.3 / 16.2	41.5 / 43.3	119.3 / 163.2

Table 3: Average and Standard Deviation Change in MPC Performance with Bias Corrected Forecasts.

Climate Zone	Electric Charge [%]	Glare Index [%]	Daylight Ratio [%]
1A	-0.2 / 0.4	**4.3 / 3.5**	-0.9 / 2.6
2A	0.0 / 0.2	2.3 / 6.3	0.4 / 2.1
2B	**0.4 / 0.8**	2.3 / 1.9	4.2 / 3.3
3A	0.1 / 0.4	**4.8 / 4.0**	1.6 / 3.1
3B	0.2 / 0.6	2.2 / 2.4	2.7 / 2.4
3B-C	0.0 / 0.3	3.1 / 2.4	1.5 / 4.0
3C	-0.1 / 0.3	2.7 / 2.6	1.0 / 3.1
4A	0.0 / 0.3	3.4 / 2.8	0.1 / 2.8
4B	**0.2 / 0.9**	2.5 / 2.9	4.4 / 4.2
4C	**-0.3 / 1.5**	**3.5 / 3.3**	1.2 / 2.8
5A	-0.2 / 0.4	2.8 / 4.3	3.3 / 6.8
5B	0.2 / 0.4	3.2 / 7.1	3.6 / 4.4
6A	0.0 / 0.3	3.2 / 3.5	**11.4 / 20.5**
6B	-0.1 / 0.8	2.4 / 2.5	**5.9 / 4.8**
7	-0.1 / 0.2	2.5 / 3.1	**10.3 / 14.3**
All	0.0 / 0.6	3.0 / 3.7	3.4 / 7.8

showed that bias correction removes most of the performance changes caused by the forecast inaccuracy. Electric charges with bias-corrected stochastic forecasts were very similar to simulations with perfect forecasts. The average glare index was only 3.0 % higher with bias-corrected forecasts, compared to 41.5 % higher with stochastic forecasts that did not include bias correction. Since the MPC re-evaluates the control strategy every five minutes and bias correction removes the error at the current time, the MPC is able to use forecasts with very small errors for the current time. For example, without bias correction an inaccurately low GHI forecast for the current time leads the MPC to under-predict glare, brighten the windows, and create uncomfortable conditions in the space.

Implementing bias correction for OAT should be manageable as temperature sensors are inexpensive and could easily be added to an MPC. Many buildings already include OAT measurements for their HVAC systems. Bias correction for irradiation is less straightforward. Accurate irradiation sensors are expensive and require regular cleaning, increasing installation cost and decreasing MPC performance in cases where the sensors are not adequately maintained. Cloud cover sensors are less expensive and would enable estimating solar irradiation, but still require regular cleaning. Hedegaard *et al.* proposed a method of estimating the local weather conditions using measurements from several nearby weather stations.

This would provide a no-hardware and no-maintenance approach which could effectively provide bias correction. This method may struggle to estimate irradiance on partly-cloudy days, as the nearby weather stations may be experiencing different solar conditions from the controlled building. Further research is needed to evaluate the benefits and costs of these different solutions.

This study focused on the impacts of weather forecast uncertainty and bias correction on MPC performance for dynamic facades in small office spaces. Further research is needed to evaluate the impacts in different cases. Impending work will perform the analysis on the same building with the MPC controlling both the dynamic facade and the HVAC system. Other valuable research projects will include performing similar analyses on different buildings, such as large offices or institutional buildings, or buildings with other hardware, such as thermal energy storage or electric water heaters.

Conclusion

This paper (a) evaluated the accuracy of HRRR weather forecasts in the contiguous United States, (b) introduced a novel stochastic algorithm adding typical error to weather forecasts, and (c) evaluated the impact of weather forecast error and bias correction on the performance of model predictive controls for dynamic facades. The uncertainty in weather forecasts decreased the performance of the control system in terms of both en-

ergy cost and occupant comfort. Bias correction largely eliminated the error in weather forecasts enabling the full potential of predictive control systems, but practical deployment methods are not yet readily available. While temperature correction can likely be achieved using readily-available sensors, further research is needed to develop solutions to correct solar irradiance forecasts.

Acknowledgment

References

DarkSky. 2021. Dark Sky by Apple. https://darksky.net. Accessed 12/21/2021.

Gehbauer, Christoph, David H Blum, Taoning Wang, and Eleanor S Lee. 2020. "An assessment of the load modifying potential of model predictive controlled dynamic facades within the California context." *Energy and Buildings* 210:109762.

Griffin, Sarah M, Jason A Otkin, Christopher M Rozoff, Justin M Sieglaff, Lee M Cronce, Curtis R Alexander, Tara L Jensen, and Jamie K Wolff. 2017. "Seasonal analysis of cloud objects in the High-Resolution Rapid Refresh (HRRR) model using object-based verification." *Journal of Applied Meteorology and Climatology* 56 (8): 2317–2334.

Hagedorn, R., T. M. Hamill, and J. S. Whitaker. 2008. "Probabilistic forecast calibration using ECMWF and GFS ensemble forecasts. Part I: Two-meter temperatures." *Monthly Weather Review*.

Hedegaard, Rasmus Elbæk, Theis Heidmann Pedersen, Michael Dahl Knudsen, and Steffen Petersen. 2018. "Towards practical model predictive control of residential space heating: Eliminating the need for weather measurements." *Energy and Buildings* 170:206–216.

Holmgren, William F., Clifford W. Hansen, and Mark Mikofski. 2018. "pvlib python: a python package for modeling solar energy systems." Journal of Open Source Software." *Journal of Open Source Software*.

Killian, Michaela, and Martin Kozek. 2016. "Ten questions concerning model predictive control for energy efficient buildings." *Building and Environment* 105:403–412.

Larson. 2016. "Day-ahead forecasting of solar power output from photovoltaic plants in the American Southwest." *Renewable Energy 91*.

Lee, Temple R, Michael Buban, David D Turner, Tilden P Meyers, and C Bruce Baker. 2019. "Evaluation of the High-Resolution Rapid Refresh (HRRR) model using near-surface meteorological and flux observations from northern Alabama." *Weather and Forecasting* 34 (3): 635–663.

Maxwell, Eugene L. 1987. "A Quasi-Physical Model for Converting Hourly Global Horizontal to Direct Normal Insolation." *Solar Energy Research Institute*.

Oldewurtel, Frauke, Alessandra Parisio, Colin N Jones, Dimitrios Gyalistras, Markus Gwerder, Vanessa Stauch, Beat Lehmann, and Manfred Morari. 2012. "Use of model predictive control and weather forecasts for energy efficient building climate control." *Energy and Buildings* 45:15–27.

Petersen, Steffen, and Katrine Wieck Bundgaard. 2014. "The effect of weather forecast uncertainty on a predictive control concept for building systems operation." *Applied Energy* 116:311–321.

Rogers, Matt, Steve Miller, Cindy Combs, S Benjamin, C Alexander, M Sengupta, Jan Kleissl, and Patrick Mathiesen. 2012. "Validation and analysis of HRRR insolation forecasts using SURFRAD." *Proceedings of the American Solar Energy Society, Rayleigh, NC*.

Široký, Jan, Frauke Oldewurtel, Jiří Cigler, and Samuel Prívara. 2011. "Experimental analysis of model predictive control for an energy efficient building heating system." *Applied energy* 88 (9): 3079–3087.

SURFRAD. 2022. SURFRAD Overview: Surface Radiation Budget Monitoring. https://gml.noaa.gov/grad/surfrad/overview.html. Accessed: 1/6/2022.

Werth, D., and A. Garret. 2011. "Patterns of Land Surface Errors and Biases in the Global Forecasrt System." *American Meteorological Society*.

Weygandt, et al. 2009. "The High Resolution Rapid Refresh (HRRR): An hourly updated convection resolving model utilizing radar reflectivity assimilation from the RUC/RR." *23rd Conf. on Weather Analysis and Forecasting/19th Conf. on Numerical Weather Prediction*. Amer. Meteor. Soc., Omaha, NE.